Transactions of the Korean Nuclear Society Spring Meeting
Jeju, Korea, May 12-13, 2016

Crud and Oxide Layer Modeling for Safety Analysis of a PWR

Joosuk Lee and Gwanyoung Kim
Korea Institute of Nuclear Safety
62 Gwahak-ro, Yusong-gu, Daejeon, 305-338, Republic of Korea
Tel: +82-42-868-0784, Fax: +82-42-868-0045
Email: jslee2@kins.re.kr

1. Introduction

As licensed fuel burnup has increased continuously, fuel has been used at more harsh environments than previous ones. Thereby, the thickness of oxide layer, which was formed on the outer surface of zirconium alloy cladding during normal operation, has reached about 80 μm even in use of the improved cladding alloy. Further, sufficient amount of crud buildup can take place on the cladding surface, for example, due to the replacement of steam generator in primary coolant circuit, and if combined with boron precipitation, this possibly can result in the crud indued power shift. Actually, several power shift events have been taking place at domestic nuclear power plants. It was analyzed that for the occurrence of crud induced power shift, required minimum thickness of crud was about 30 μm [1]. Thus, we can deduce that the accumulated crud can be possibly thick enough if some given conditions are met in the operating plants.

Oxide and crud layer on the cladding surface will behavior as a thermal barrier due to their lower thermal conductivity. And apparently it will increase the stored energy during steady-state operation, and heat conduction from fuel to coolant will be inhibited during transient also. However, such detrimental effects of oxide and crud layer were not factorized in the modeling of fuel for the assessment of deterministic safety analysis, such as reactivity-initiated accidents(RIAs) and loss-of-coolant accidents (LOCAs).

In this paper, simple models for the calculation of thermal conductivity and heat capacity of crud were established. And well known models of conductivity and heat capacity of oxide were also adapted. Based on these models, FRAPTRAN-1.5 fuel performance code was modified. And impacts of these on the RIA and LOCA safety analysis have been analyzed.

2. Analysis Details

2.1 Crud and oxide model

2.1.1 Crud model

For the establishment of simple crud models, following assumptions were made.

- Crud is a porous media that is composed of solid phase and liquid water(or steam or mixture of water and steam), and there is no directionality between two phases.
- Average volume fraction of solid in the crud is assumed as 0.5 with the linear fractional change from +0.1 to -0.1(from bottom to top surface of the crud).
- Solid phase crud is composed of NiO, $NiFe_2O_4$ and Fe_3O_4 with the volume fraction of 0.15, 0.75 and 0.1, respectively. Thermal conductivity and specific heat of each phase is listed in Table 1.
- At forced convection, subcooled nucleate and saturated heat transfer condition, if crud temperature exceeds the saturation temperature of water at the given pressure, it is assumed that 10 vol. % of steam phase is encapsulated in the crud. And the temperatures of steam and liquid phase are set to just above and below the saturation temperature, respectively.
- At the film boiling and super heated heat transfer condition, super heated steam occupies in the crud layer instead of water.

Based on the above assumptions, thermal conductivity of crud(k_{Crud}) is calculated by the following relationships.

$$k_s = 0.15k_{s\_NiO} + 0.75k_{s\_NiFe_2O_4} + 0.1k_{s\_Fe_3O_4}$$

$$k_{Crud\_\max} = \varepsilon k_s + (1-\varepsilon)k_w$$

$$k_{Crud\_\min} = \left(\varepsilon / k_s + (1-\varepsilon)/k_w\right)^{-1}$$

$$k_{Crud} = \left(0.5/k_{Crud\_\max} + 0.5/k_{Crud\_\min}\right)^{-1}$$

where,
k_w = thermal conductivity of water(or steam or mixture)
k_{Crud_max} = maximum thermal conductivity(parallel case)
k_{Crud_min} = minimum thermal conductivity(serial case)
ε = volume fraction of solid phase of crud
k_{Crud} = crud thermal conductivity

Specific heat of crud(Cp_{Crud}) is calculated based on the following relationships.

$$\rho_s Cp_s = 0.15\rho_{NiO}Cp_{NiO} + 0.75\rho_{NiFe_2O_4}Cp_{NiFe_2O_4} + 0.1\rho_{Fe_3O_4}Cp_{Fe_3O_4}$$

$$\rho_{ave}Cp_{Crud} = \varepsilon\rho_s Cp_s + (1-\varepsilon)\rho_w Cp_w$$

where,
Cp_{Crud} = specific heat of crud
Cp_s, Cp_w = specific heat of solid and water(or steam or mixture),
Cp_{NiO}, $Cp_{NiFe2O4}$, Cp_{Fe3O4} = specific heat of NiO, $NiFe_2O_4$

Table 1. Thermal conductivity and specific heat of solid phase of crud and zirconium oxide

Specious	Thermal conductivity, W/m-k	Specific heat capacity, J/kg-K
NiO	$-5.602x10^{-9}T^3 + 2.435x10^{-5}T^2-0.03543T+21.658$ [2]	Data from R.J Radwanska and Z. Ropka[3]
$NiFe_2O_4$	$1/(4.3711x10^{-4} + 2.7512x10^{-2}T)$ [4]	$-1.2057+(1.1411\cdot10^{2})T-(2.4950\cdot10^{5})T^2+(2.4611\cdot10^{8})T^3-(8.8726\cdot10^{12})T^4$ $(298<T<823)$ [4] $-6.5674+(3.2540\cdot10^{2})T-(5.0578\cdot10^{5})T^2+(3.3300\cdot10^{8})T^3-(7.9139\cdot10^{12})T^4$ $(923<T<1373)$ [4]
Fe_3O_4	Data from Yasuo and Keiji Naito [5]	Data from Chase [6]
ZrO_2	$1.9599-T(2.41x10^{-4}-T(6.43x10^{-7}-T1.946x10^{-10}))$[7]	MATPRO [8]

and Fe_3O_4

ρ_{NiO}, $\rho_{NiFe2O4}$, ρ_{Fe3O4} = density of NiO, $NiFe_2O_4$ and Fe_3O_4

ρ_s, ρ_w , ρ_{ave} = solid, water(or steam or mixture) and average density of crud

2.1.2 Oxide model

Models of thermal conductivity and specific heat of zirconia(ZrO_2) are adapted from well known FRAPCON and MATPRO model, respectively[7, 8].

2.2 Analyzed safety analysis conditions

For the implementation of oxide and crud model, finite difference method was used for the temperature calculation. For this, FRAPTRAN-1.5 code was modified. 5 evenly spaced radial nodes were allocated to oxide and crud layer. Westinghouse-type 17x17 fuel with Zircaloy-4 cladding was utilized. Design parameters of fuel rod, operating conditions, and base irradiation power history were obtained from NUREG-1754[9].

Impacts of those layers to the RIA and LOCA safety analysis were assessed. Initiation of RIA and LOCA were supposed to occur at the fuel burnup of 30MWd/kgU. Axially maximum oxide thickness at that burnup was 26 μm and imposed thickness of crud was 30 μm. Both hot zero power(HZP) and hot full power(HFP) RIA were analyzed. Injected energy was about 100 cal/g. Large break loss-of-coolant accident(LBLOCA) was analyzed by factorizing the models also. Detailed analysis conditions can be found in author's previous work[10-12]. Coding error in calculation of volumetric weight in FRAPTRAN-1.5 was fixed.

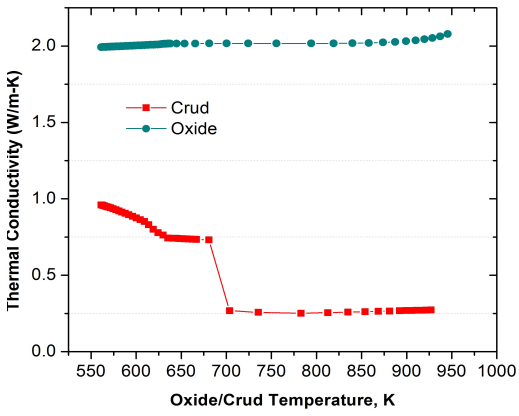

Fig. 1. Effective thermal conductivity of crud and oxide as a function of temperature at 15.5MPa coolant pressure. Crud thickness = 30 μm.

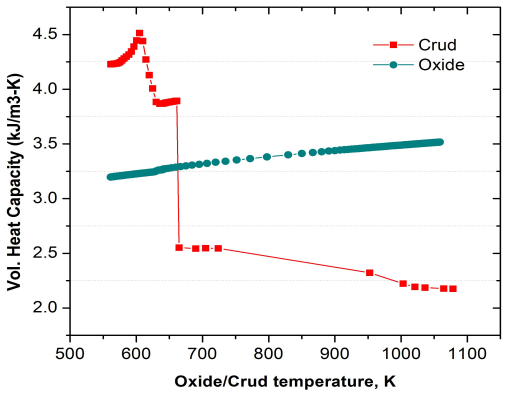

Fig. 2. Volumetric heat capacity of crud and oxide as a function temperature at 15.5 MPa. 30 μm thickness of crud.

3. Results

3.1 Physical properties of crud and oxide

3.1.1 Thermal conductivity

Evaluated effective thermal conductivity of crud and oxide is shown in Fig. 1. Thermal conductivity of crud is 0.96 W/m-K at 561K, and as temperature increased it reduced continuously until saturated at 0.74 W/m-K. The saturation was due to the assumption of crud temperatures at subcooled nucleate and saturate boiling condition. These conductivity values are well within the experimentally determined values of crud in boiling cases. It was ranging from 0.519 to 1.39 W/m-K[13]. As heat transfer mode changed to film boiling and super heated condition, thermal conductivity reduced abruptly to 0.24 W/m-K due to the complete intrusion of steam phase in the crud. Thermal conductivity of oxide is about 2 W/m-K irrespective of temperature.

3.1.2 Heat capacity

Fig. 2 shows the effective volumetric heat capacity with temperature change. Heat capacity of crud was 4.24 kJ/m^3-K at 561K. And it increased slightly up to 4.56 kJ/m^3-K and reduced continuously until saturated at around 3.8 kJ/m^3-K. As heat transfer mode entered into the film boiling, abrupt drop of heat capacity was observed. Meanwhile, heat capacity of oxide is slightly increased from 3.19 to 3.51 kJ/m^3-K as temperature changed from 561 to 1058 K.

3.2 RIA safety analysis

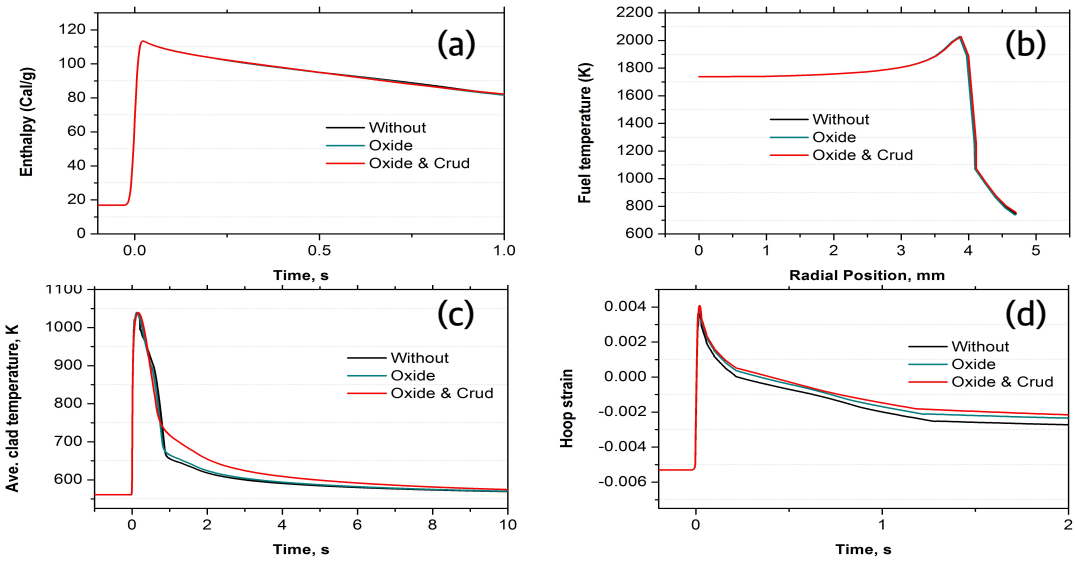

Fig. 3. Evolution of (a) fuel enthalpy, (c) average cladding temperature and (d) hoop strain at peak node, and (b) distribution of peak fuel temperature inside of fuel at the HZP RIA condition. FWHM = 20ms.

3.2.1 HZP condition

Fig. 3 shows the fuel performance change with consideration of crud and oxide layer in a HZP RIA analysis. Fig.3(a) and (b) shows the peak fuel enthalpy and peak fuel temperature, and they are not changed by the oxide and crud layer. Fig. 3(c) and (d) shows the evolution of average cladding temperature and hoop strain, respectively. Peak cladding temperature and maximum hoop strain were almost same, but some differences were discovered as time progressed. However the differences were small. These relatively small impacts may be due to the very short period of power excursion and zero power condition before RIA. In this analysis considered full width half maximum(FWHM) was 20 ms, thereby fuel behaviors almost adiabatically.

3.2.2 HFP condition

Fig. 4 shows the fuel performance evolution at HFP RIA condition. Fig. 4(a) and (b) show the evolution of enthalpy and fuel centerline temperature. As oxide and oxide + crud layer were considered, changes of peak fuel enthalpy with respect to the bare cladding case

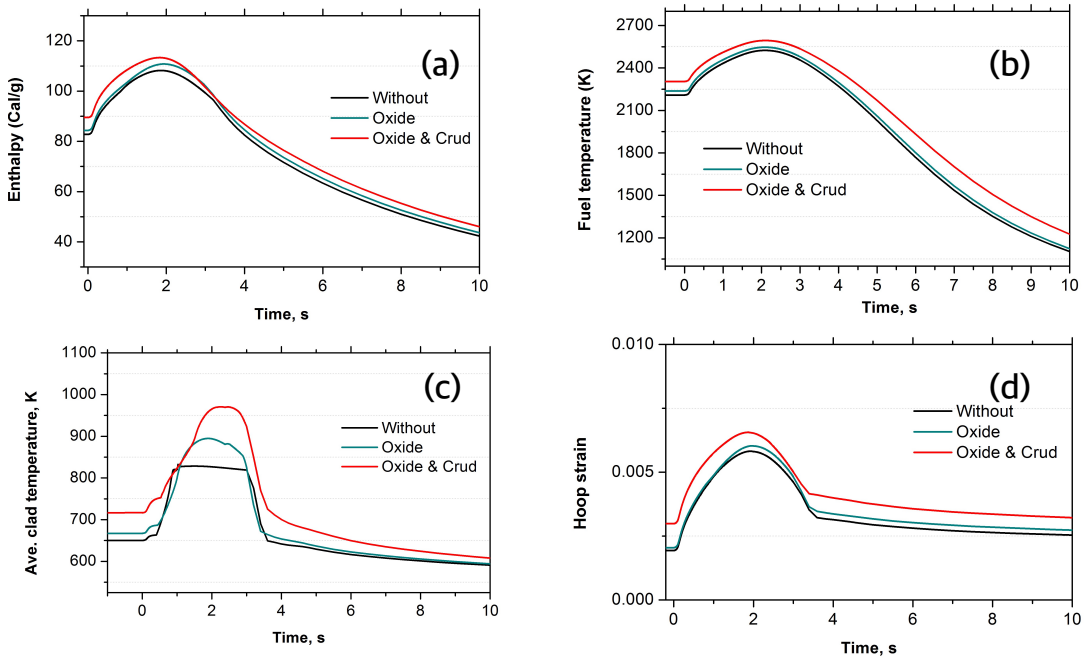

Fig. 4. Evolution of (a) fuel enthalpy, (b) fuel temperature, (c) average cladding temperature and (d) hoop strain at peak node at HFP RIA condition.

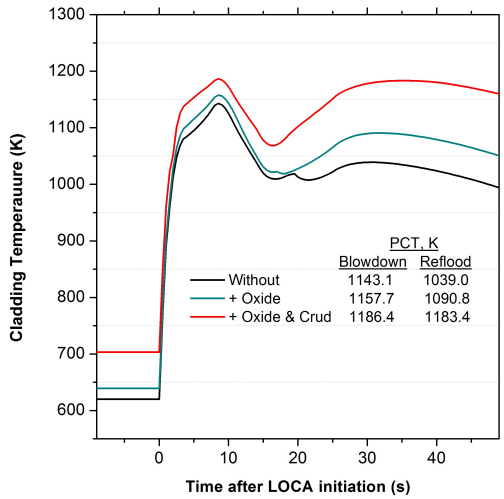

Fig. 5. Cladding temperature evolution at LBLOCA condition with oxide and crud layer consideration.

were 2.58 and 5.12 cal/g, and changes of maximum fuel centerline temperature were 22.4 and 70K, respectively. Fig. 4(c) and (d) show the evolution of average cladding temperature and hoop strain. As oxide and oxide + crud layer were considered, peak cladding temperature increased by 66.3 and 142.3K, respectively. And maximum hoop strain increased by 0.02 and 0.07%. These performance results indicate that the impacts of oxide and crud layer in the HFP RIA safety analysis are relatively stronger than the HZP condition.

3.3 LOCA safety analysis

Fig. 5 shows the cladding temperature evolution with the consideration of crud and oxide layer in LBLOCA safety analysis. As oxide layer considered alone the blowdown and reflood PCT increased by 14.6 and 51.8 K, respectively. But as oxide and crud layer considered altogether, blowdown and reflood PCT increased by 43.3 and 144.4K, respectively. These amounts are significant.

3.4 Further works

Improvement of proposed crud model is necessary. For example, roles of chimney and amount of steam encapsulation in the crud layer need to be clarified. And uncertainties related to the crud and oxide, and their effects to the safety analysis have to be evaluated.

4. Summary

Modeling of crud and oxide layer for the deterministic safety analysis of a PWR was carried out. Based on this, RIA and LOCA safety analysis have been done. Followings are summary of this work.

- Assessed thermal conductivity and heat capacity of crud layer showed reasonable values as compared with the experimental results.
- Fuel performance changes after the factorization of crud and oxide layer in a HZP RIA safety analysis were small. But, in a HFP condition fuel performances were affected relatively strongly.
- Peak cladding temperature in a LOCA safety analysis was affected significantly by the crud and oxide layer.

REFERENCES

1. Henshaw, J., McGurk, J.C., Sims, H.E., Tuson, A., Dickinson, S., Deshon, J., 2006. A model of chemistry and thermal hydraulics in PWR fuel crud deposits. J. Nucl. Mater. 353, 1–11.
2. Kingery, Francl, Coble, Vasilos, J. Am. Ceram. Soc. 37(2)(1954) 107-111.
3. R.J. Radwanski, and Z. Ropka, “Specific Heat and the Ground State of NiO “, ACTA PHYSICA POLONICA A No.1, Vol. 114 (2008)
4. A.T. Nelson et. al., Thermal Expansion, Heat Capacity and Thermal Conductivity of Nickel Ferrite ($NiFe_2O_4$), Journal of the American Ceramic Society, MIT open access article, 2013
5. Yasuo Noda and Keiji Naito, “The Thermal Conductivity and Diffusivity of MnxFe3-xO4 (0<x<1.5) from 200 to 700 K, NETSUSOKUTEI 5(1) 11-18(1978)
6. Chase, M.W., Jr., NIST-JANAF Themochemical Tables, Fourth Edition, J. Phys. Chem. Ref. Data, Monograph 9, 1998
7. W.G. Luscher et. al., “Material Property Correlations: Comparison between FRAPCON-3.4, FRAPTRAN-1.4, and MATPRO”, NUREG/CR-7024, PNNL-19417, 2011
8. L.J. Siefken., “SCDAP/RELAP5/MOD3.3 Code Manual: MATPRO”, NUREG/CR-6150 Vol. IV, Rev.2, 2001
9. O’Donnell, G.M., Scott, H.H., Meyer, R.O., 2001. A New Comparative Analysis of LWR Fuel Designs. NRC, NUREG-1754.
10. Joosuk Lee, Swengwoong Woo, “Effects of fuel rod uncertainty on the LBLOCA safety analysis with limiting fuel burnup change”, *Nuclear Engineering and Design* 273 (2014) 367-375.
11. Joosuk Lee, Swengwoong Woo, “Effects of Fuel Rod Uncertainty in PWR HZP RIA Analysis”, TopFuel 2015, Zurich, Switzerland, September 13-17, 2015
12. Joosuk Lee, Swengwoong Woo, “Evaluation of Fuel Performance Uncertainty in a PWR RIA Analysis”, *Transactions of the Korean Nuclear Society Autumn Meeting, Gyeongju, Korea, October 29-30, 2015*
13. J. Deshon, Simulated Fuel Crud Thermal Conductivity Measurements Under Pressurized Water Reactor Conditions, Technical Report 1022896, EPRI, October 2011.